

Cite this: *CrystEngComm*, 2011, **13**, 5100

www.rsc.org/crystengcomm

PAPER

# Morphology effect on the luminescent property and antibacterial activity of coordination polymer particles with identical crystal structures†

Kuaibing Wang, Zhirong Geng, Yuxin Yin, Xiaoyan Ma and Zhilin Wang\*

Received 14th February 2011, Accepted 20th May 2011

DOI: 10.1039/c1ce05202k

Four different morphologies of coordination polymer particles (CPPs) with identical structures, which have effects on their luminescent properties and antibacterial activities, have been synthesized. We accounted for the possible formation mechanisms of the different morphologies from the molecular level. The additives such as Et<sub>3</sub>N and acetic acid play an important role in the particle formation rate by means of manipulating the deprotonation rate of the organic linker and thus the particle size and shape. Meanwhile, in our future research work, we need to take the morphology effect into consideration.

## 1. Introduction

Coordination polymer particles (CPPs) have attracted growing interest in chemistry and material science due to their highly tailorable properties and potential use in a variety of important applications, such as gas storage,<sup>1</sup> catalysis,<sup>2</sup> ion exchange,<sup>3</sup> optics,<sup>4</sup> and drug delivery.<sup>5</sup> In contrast with the field of metal-organic framework materials (MOFs), which has been investigated over the past two decades, the field of CPPs is at an early stage, however, the size- and morphology-dependent properties can make them attractive for a number of biomedical applications where conventional MOFs are not ideal because of their bulk size and static structures.<sup>6</sup> In this regard, Horcajada *et al.* found that the nanoparticles of the coordination polymers were ideal candidates for a new valuable solution in the field of drug-delivery systems.<sup>7</sup> In addition, there are now all kinds of ways of synthesizing CPPs from a wide class of metal salts and organic ligands which can assemble together *via* coordination chemistry principles.<sup>8–10</sup> In these methods, the synthetic processes of CPPs are much more rapid than MOFs whose synthetic processes can even take 1/2 day to multi-day procedures.<sup>11–13</sup> Furthermore, the coordination polymer particles also show advantages over the classic metal oxide or carbon based materials, such as easier synthetic procedures and the fact that their magnetic, gas-sorption and optical properties can be modified by purposefully selecting the building blocks.

Thus far, the crystal-growth mechanism of CPPs has rarely been discussed because it is difficult to modulate the rate of

framework extension.<sup>14,15</sup> Controlling the growth-rate between metal ions and organic linkers, so-called “coordination equilibrium”, is important when varying the crystal features of CPPs, such as their size and morphology.<sup>15</sup> In this strategy, we documented the use of additives such as Et<sub>3</sub>N and acetic acid to modulate the rate of interactions by controlling the deprotonation rate of the organic linker and consequently the particle size and shape. Recent studies revealed that some metal oxide and metal particles possess high antibacterial activity.<sup>16,17</sup> However, many of these nanomaterials have shown severe cytotoxicity,<sup>18,19</sup> which restricts a range of medical and environmental applications. In contrast with these conventional nanoparticle analogues, CPPs are constructed from molecules, rather than atoms,<sup>6</sup> which may be suitable for using in the antibacterial field due to their low toxicity, biocompatibility and biodegradability.<sup>7</sup> As to the function of CPPs, much more attention has been devoted to study the difference in gas-uptake properties of CPPs with the different morphologies due to their differences in porosities and surface areas.<sup>1,6,15</sup> Interestingly, however, none of these studies address whether the different morphologies with the identical structure have effects on the physical property or bioactivity. Considering this strategy, herein, the different morphologies of coordination polymer particles have been easily prepared by mixing 4,4'-dicarboxy-2,2'-bipyridine (H<sub>2</sub>dcbp) and Cu(OAc)<sub>2</sub> in mixed solvents of water and ethanol with vigorous stirring. In addition, we also investigate the luminescent properties and antibacterial activities of CPPs with different morphologies in the experimental process.

H<sub>2</sub>dcbp can act as an O,N-bifunctional ligand where the pyridine nitrogen atoms are apt to bridge a metal ion, and the carboxylic acid either forms self-complementary hydrogen bonds to neighbouring ligands, or coordinates directly to adjacent metal ions following deprotonation. The ligand can react with the different cupric salts to obtain the same crystal structure regardless of adding a certain amount of glacial acetic acid (HAc) or NaOH to adjust the pH value.<sup>20,21</sup> In this paper, we obtained

State Key Laboratory of Coordination Chemistry, Coordination Chemistry Institute, Nanjing National Laboratory of Microstructures, Nanjing University, Nanjing, 210093, P. R. China. E-mail: wangzl@nju.edu.cn

† Electronic supplementary information (ESI) available: Experimental procedures, Fig. S11–S15 showing FT-IR spectra, EDX spectra, possible formation mechanism of CPP-1a, SEM images of CPP-1d and CPP-1c and XRD pattern of CPP-1c of adding different additives. See DOI: 10.1039/c1ce05202k

four different morphologies under different reaction conditions with identical structures, namely, rhombus layer (CPP-1a), rhombus disk (CPP-1b), rhombus lump (CPP-1c) and bread-like (CPP-1d), respectively.

## 2. Experimental

### Preparation of coordination polymer particles

**Synthesis of rhombus layer (CPP-1a).** Cu(OAc)<sub>2</sub> (0.011 g) and H<sub>2</sub>dcbp (0.012 g) with a molar ratio about 1 : 1 were mixed in 20 mL H<sub>2</sub>O/CH<sub>3</sub>CH<sub>2</sub>OH (v:v, 1 : 1) under vigorous stirring, and triethylamine (Et<sub>3</sub>N, 40 μL) was added 5 min later. The solution was then kept still for 4 h at room temperature, and the solid material was collected by centrifugation and washed with water and CH<sub>3</sub>CH<sub>2</sub>OH for three times. Anal. calc. for CuC<sub>12</sub>H<sub>14</sub>N<sub>2</sub>O<sub>8</sub>: C, 38.15; H, 3.74; N, 7.41%. Found: C, 37.97; H, 3.54; N, 7.29%.

**Synthesis of rhombus disk (CPP-1b).** An identical procedure with CPP-1a was followed to prepare CPP-1b except the temperature was changed from R.T. to 70 °C. Anal. calc. for CuC<sub>12</sub>H<sub>14</sub>N<sub>2</sub>O<sub>8</sub>: C, 38.15; H, 3.74; N, 7.41%. Found: C, 38.39; H, 3.29; N, 7.35%.

**Synthesis of rhombus lump (CPP-1c).** CPP-1c was prepared by the same procedure of CPP-1a except that Et<sub>3</sub>N was replaced by CH<sub>3</sub>COOH (HAc, 2 mL). Anal. calc. for CuC<sub>12</sub>H<sub>14</sub>N<sub>2</sub>O<sub>8</sub>: C, 38.15; H, 3.74; N, 7.41%. Found: C, 37.99; H, 3.45; N, 7.29%. Found: C, 38.87; H, 3.36; N, 7.18%.

**Synthesis of bread-like (CPP-1d).** An identical procedure with CPP-1a was followed to prepare CPP-1d except the sodium dodecylsulfonate (SDS, 0.02 g) was added in the reaction system. Anal. calc. for CuC<sub>12</sub>H<sub>14</sub>N<sub>2</sub>O<sub>8</sub>: C, 38.15; H, 3.74; N, 7.41%. Found: C, 40.02; H, 3.64; N, 7.32%.

### Antibacterial test

The antibacterial activity of the synthesized CPPs was tested against *B. subtilis*, *S. aureus*, *S. enteritidis*, *E. coli*, *P. vulgaris* and *P. aeruginosa* by determining the minimum inhibitory concentrations (MICs, μg mL<sup>-1</sup>) through a colorimetric method using the dye MTT (3-(4,5-dimethylthiazol-2-yl)-2,5-diphenyltetrazolium bromide). Firstly, the stock solution of the synthesized samples (50 μg mL<sup>-1</sup>) were prepared in dimethyl sulfoxide (DMSO) and graded quantities of the test crystals were incorporated in a specified quantity of sterilized liquid medium. Secondly, the solutions were poured into microtitration plates, and then a suspension of the microorganism with concentration of approximately 10<sup>5</sup> cfu mL<sup>-1</sup> was added. After incubation at 37 °C for 24 h, 50 μL of PBS (phosphate buffered saline 0.01 mol L<sup>-1</sup>, pH 7.4: Na<sub>2</sub>HPO<sub>4</sub>·12H<sub>2</sub>O 2.9 g, KH<sub>2</sub>PO<sub>4</sub> 0.2 g, NaCl 8.0 g, KCl 0.2 g, distilled water 1000 mL) containing 2 mg mL<sup>-1</sup> of MTT was added to each well. Incubation was continued at room temperature for 4–5 h, followed by the addition of 100 μL of isopropanol containing 5% 1 mol L<sup>-1</sup> HCl to extract the dye. In the end, the optical density (OD) was measured with a microplate reader at 570 nm to determine the MICs.

### General methods

Elemental analyses of C, H, and N were performed on an Elementar Vario MICRO Elemental Analyzer at the Analysis Centre of Nanjing University. Fourier-transform infrared (FT-IR) spectra were obtained on a Bruker Vector 22 FT-IR spectrophotometer by using KBr pellets. Thermogravimetric and differential thermal analyses (TG-DTA) were performed in a N<sub>2</sub> atmosphere (a flow rate of 100 mL min<sup>-1</sup>) on a simultaneous SDT 2960 thermal analyzer from 25 °C up to 600 °C, with a heating rate of 10 °C min<sup>-1</sup>. X-ray powder diffraction (XRPD) data were collected on a Bruker D8 Advance instrument using Cu-Kα radiation (λ = 1.54056 Å) at room temperature. The morphology of the as-prepared samples and the corresponding energy dispersive X-ray (EDX) spectroscopy were obtained by using a Hitachi S-4800 field-emission scanning electron microscope (FE-SEM). Transmission electron microscopy (TEM) images were captured on the JEM-2100 microscopy instrument at an acceleration voltage of 200 kV. The adsorption isotherm of nitrogen was measured at 77 K by using Micromeritics ASAP 2020 M + C volumetric adsorption equipment.

## 3. Results and discussion

The structures of all these coordination polymer species are supported by X-ray powder diffraction (XRD) results as shown in Fig. 1. All the diffraction of these species can be readily indexed to the bulk-crystals that were reported previously by Tynan *et al.*<sup>20</sup> This result suggests that they are isostructural. The same chemical composition of CPP-1a–CPP-1d was also confirmed by elemental analysis (EA), infrared spectroscopy (IR) and energy dispersive X-ray (EDX) spectroscopy (see Experimental section, Fig. S11 and S12 in the ESI†). EDX confirms that the resulting samples are composed of Cu, C, N and O, and the atomic ratios for C : N are all near 5 : 1, in agreement with the results of elemental analysis.

In the experimental process, we used triethylamine (Et<sub>3</sub>N) as a basic additive to deprotonate the organic building blocks (H<sub>2</sub>dcbp) at room temperature (R.T.) (Scheme 1). As a result, the

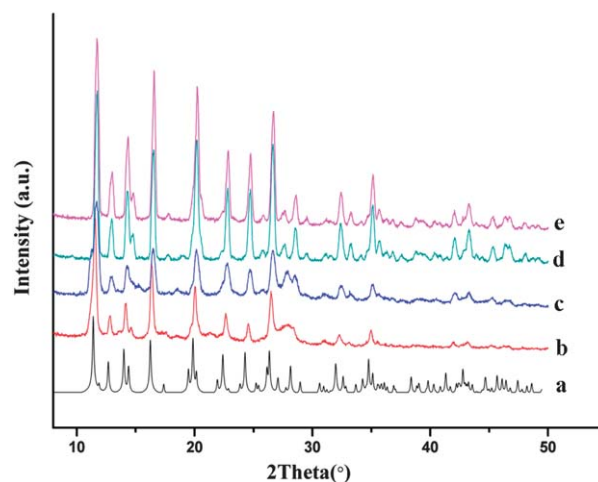
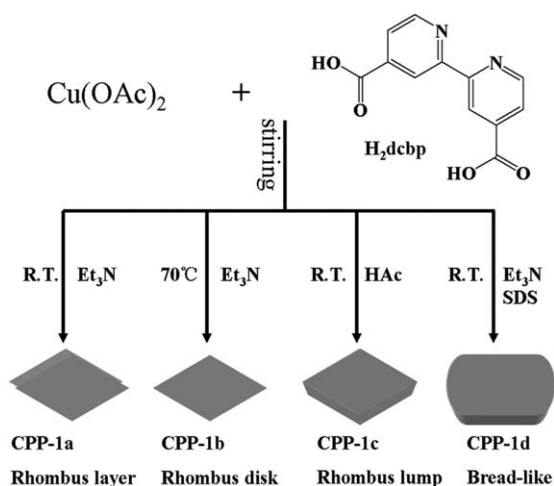


**Fig. 1** (a) A simulated XRD curve based on the published structure of Tynan *et al.* and XRD patterns of (b) CPP-1a (c) CPP-1b (d) CPP-1c (e) CPP-1d.



**Scheme 1** Preparation of rhombus-like and bread-like coordination polymer particles.

rhombus layer morphology was maintained on a large scale as shown in Fig. 2a. The average size of the width was determined by field-emission scanning electron microscopy (SEM) to be  $2.40 \pm 0.16 \mu\text{m}$  (Fig. 2b). Fig. 2c indicates that the thickness of CPP-1a is about 600 nm. The possible reason of forming the rhombus layer morphology seems to be explained by the crystal structure as shown in Fig. 2d. Numbers of Cu nuclei surrounded the organic linkers to form crystal seeds, self-assembling into a rhombus-like 2-D (two-dimensional) metal-carboxylate sheet. With the reaction proceeding, the two neighbouring 2-D motifs were parallel to each other and further connected into the formation of the 3-D layer network, with the aid of hydrogen bond interactions with the water molecules.<sup>22</sup> The possible mechanism is vividly depicted in Fig. SI3 (ESI<sup>†</sup>).<sup>23</sup> When we varied the reaction temperature from R.T. to 70 °C, the rhombus disk morphology was obtained with an average size of  $2.84 \pm 0.22 \mu\text{m}$  as depicted in Fig. 3a–b. It is notable that the average size was larger with respect to CPP-1a. Furthermore, the surface

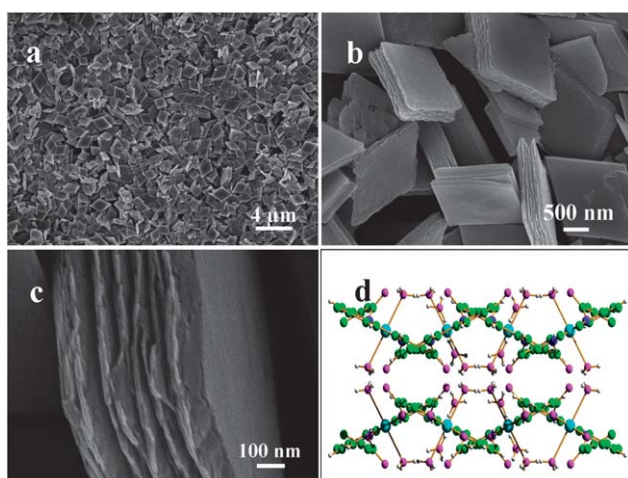


**Fig. 2** (a)–(c) SEM images of rhombus layer morphology; (d) 3-D crystal structure based on the published structure of Tynan *et al.* The lattice water molecules in the channel are presented here by red balls.

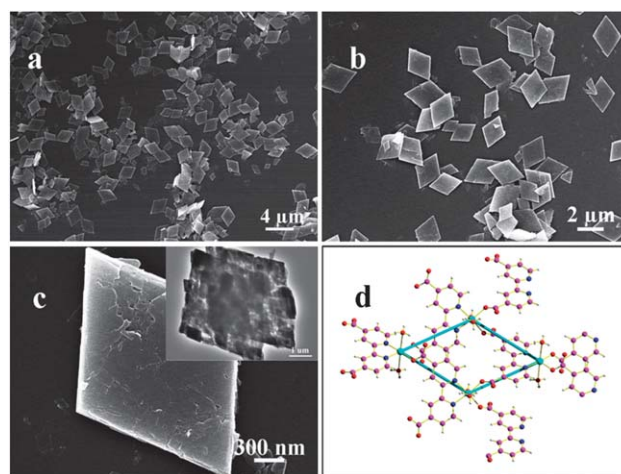


**Fig. 3** (a)–(c) SEM images of rhombus disk morphology; (d) 2-D crystal structure based on the published structure of Tynan *et al.* (inset: TEM image of rhombus disk).

was not smooth as there are some fissures on it as clearly depicted in Fig. 3c, suggesting that the rhombus disk might be composed of nanoparticles. This can be proved by the transmission electron microscopy (TEM) image on the right side of Fig. 3c, showing the nano-sized rhombic particles were assembled to the larger-sized rhombic block in the self-assembly process. It can also be explained through analyzing the crystal structure. As vividly shown in Fig. 3d, the possible reason of forming the single-layer morphology could indicate that lattice water molecules in the channel and the coordinated water molecules were all evaporated as the reaction temperature went up to 70 °C, and consequently, the crystal seeds were inclined to form the larger 2-D disk morphology rather than a 3-D network in the absence of non-covalent interactions. Although the morphology was changed from rhombus layer to rhombus disk when the reaction temperature changed, the crystal structure remained unchanged. It can be supported by thermogravimetric analysis (TGA), which revealed that the CPPs were stable up to 300 °C after an initial weight loss of 19% due to solvent liberation in the 50–100 °C temperature range (Fig. 4), which was the same as the thermogravimetric analysis of bulk-crystals. It can also be illustrated that the as-synthesized CPPs were isostructural with the bulk crystals.

Keeping the other reaction conditions unchanged comparing with CPP-1a, SDS was added into the system as a surfactant, the bread-like CPP-1d was generated as shown in Fig. SI4a (ESI<sup>†</sup>). This different morphology with larger size may be due to an incomplete packing process, resulting from the slow crystallization. The  $\text{N}_2$  adsorption isotherm measured at 77 K revealed multilayer adsorption behavior of CPP-1d (Fig. 4b). The BET and Langmuir surface areas of CPP-1d were 25.35 and 38.59  $\text{m}^2 \text{g}^{-1}$ , respectively. The  $\text{N}_2$  adsorption capacity of CPP-1d was somewhat greater than the capacity in the reported literature.<sup>24–26</sup> Notice that the  $\text{Et}_3\text{N}$  seems to act as a base to accelerate the deprotonation of the organic building blocks that constitute the coordination polymers. Besides the basic reaction conditions, we also investigated the subacidity effect on the morphology. Fortunately, the CPP-1c was generated in the presence of acetic

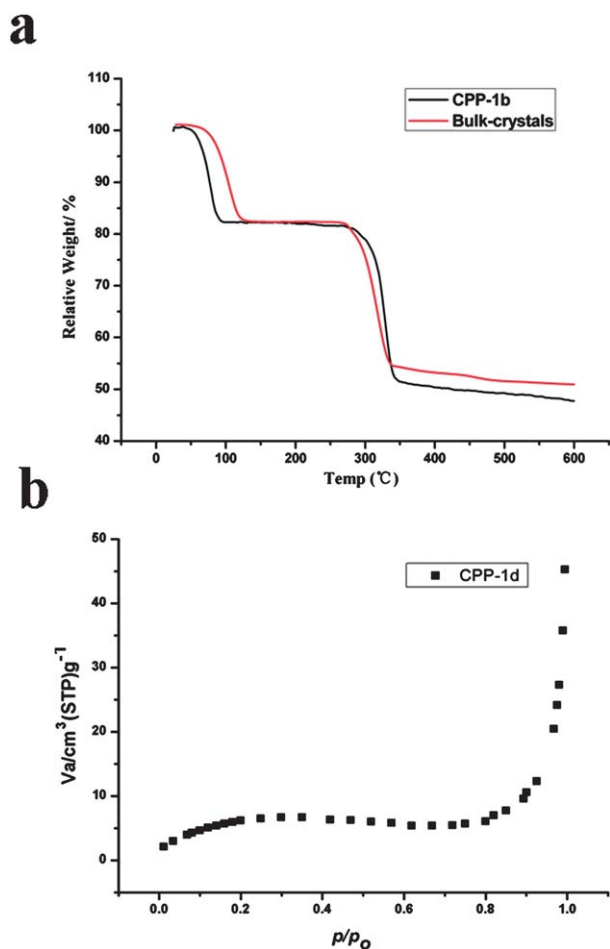


**Fig. 4** (a) TGA curves of CPP-1b and bulk-crystals. (b)  $N_2$  adsorption isotherm of CPP-1d at 77 K.

acid with the length of *ca.* 3.6  $\mu\text{m}$  (Fig. SI4b†). Viewing from Fig. 3d, acetic acid may coordinate on the surface of CPP to form strong hydrogen bonds with the backbones of the structure, leading to a decrease in the distance between two neighboring rhombic layers. Thus, the thickness of CPP-1c was 500 nm, smaller than CPP-1a. As described in other samples, acetic acid seems to delay the deprotonation rate of the building blocks resulting in the slow formation of CPPs.<sup>22</sup> We also investigated how varying the concentration of HAC affects the particle formation. When the amount of HAC was decreased from 2 mL to 1.6 mL and 1.2 mL, while the structure remained the same (Fig. SI5†), the morphology does not change remarkably, but the thickness was decreased to 480 nm and 450 nm, respectively, in contrast with CPP-1c. The result reveals that the particle size generated has a positive correlation to the amount of additives used. It is noteworthy that the  $\text{Et}_3\text{N}$  and acetic acid act as pH value controllers to adjust the particle formation rate and eventually the particle size and shape. The resulting particles were found to be stable in several solvents such as DMF, DMSO, methanol, acetic acid, pyridine and nonpolar solvents.

The photoluminescence properties of CPP-1a–CPP-1d and  $\text{H}_2\text{dcbp}$  were studied in the solid state at room temperature upon excitation at 372 nm. As shown in Fig. 5, CPP-1b, CPP-1c and CPP-1d all exhibit blue luminescence emissions at 422 nm.

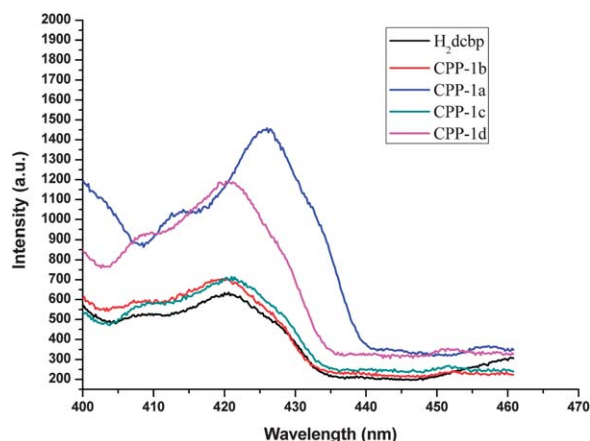


**Fig. 5** Fluorescence spectra of solid  $\text{H}_2\text{dcbp}$  and CPPs of different morphologies at room temperature.

However, CPP-1a exhibits a slight red-shift of 5 nm compared with the free  $\text{H}_2\text{dcbp}$  ligand. Taking the emission bands of the free organic ligand into consideration, the emissions of 1a–1d may be attributable to intraligand ( $\pi$ – $\pi^*$ ) transition.<sup>27</sup>

It is obvious that the intensity of rhombus layer and bread-like particles were stronger than rhombus disk and rhombus lump particles, while the intensity of rhombus disk or rhombus lump particles was close to the organic ligand. These observations indicate that the morphologies of the particles do have effects on the luminescent properties. The possible reason for the different enhancement of luminescence of synthesized CPPs with identical structures may be attributed to ligand chelation to the metal center, which effectively increases the rigidity of the ligand, and the influence of different morphologies leads to different reductions of energy loss by nonradioactive decay.<sup>28</sup> Furthermore, the stronger intensities of rhombus layer and bread-like particles may be due to their high surface areas, which can more easily absorb the external excitation light and obtain high bulk densities, thus reducing light scattering to enhance their luminescent intensities.<sup>29,30</sup>

Up to now, coordination polymer particles have been widely applied in many fields, however, as far as we know, no literature has reported their antimicrobial activities. In this study, we studied the antimicrobial activities of the synthesized CPPs against *B. subtilis*, *S. aureus*, *S. enteritidis*, *E. coli*, *P. vulgaris* and *P. aeruginosa* by determining the minimum inhibitory concentrations (MIC,  $\mu\text{g mL}^{-1}$ ) through a colorimetric method using the dye MTT.<sup>31</sup> For comparison, the antimicrobial activities of the organic ligand and the different morphologies of as-synthesized CPPs have also been investigated. The results are depicted in Table 1 and demonstrate that the rhombus lump and the rhombus layer particles can kill both gram positive and gram negative bacteria well, while the ligand  $\text{H}_2\text{dcbp}$ , the bread-like and rhombus disk particles have no or rather weak antibacterial abilities to the tested five bacteria. It could be explained on the basis of chelation theory.<sup>32</sup> The ligand chelating to the metal ions tends to make the resulting complex act as a more powerful and potent bactericidal agent, killing more of the bacteria than the ligand.<sup>33</sup> When comparing antimicrobial activities against *B. subtilis*, *S. aureus*, *E. coli* with the other Cu complex in the literature, the activities of the rhombus lump were stronger than

**Table 1** MICs (minimum inhibitory concentrations) ( $\mu\text{g mL}^{-1}$ ) of the organic ligand  $\text{H}_2\text{dcbp}$  and as-synthesized CPPs<sup>a</sup>

Samples	Minimum inhibitory concentration/ $\mu\text{g mL}^{-1}$					
	Gram positive		Gram negative			
	<i>B. subtilis</i>	<i>S. aureus</i>	<i>S. enteritidis</i>	<i>E. coli</i>	<i>P. vulgaris</i>	<i>P. aeruginosa</i>
$\text{H}_2\text{dcbp}$	+	+	+	+	+	+
Rhombus layer	12.5	12.5	25	12.5	25	25
Rhombus disk	25	50	50	50	50	50
Rhombus lump	12.5	12.5	25	6.25	12.5	6.25
Bread-like	>50	>50	>50	50	>50	50

<sup>a</sup> “+” means growth.

the reported one.<sup>33</sup> Although the real mechanism of the antibacterial effect is still uncertain, it is obvious that the morphology can influence the resulting antibacterial activity. The reason for different antibacterial activities could be that the rhombus layer and rhombus lump particles were gathered by lots of rhombic sheets, these rhombic sheets and their interior structure might effectively inhibit the growth of bacteria. Meanwhile, the rhombus lump particles may show potential antibacterial use in dental materials,<sup>34</sup> stainless steel materials and so forth.

#### 4. Conclusions

In summary, a bifunctional organic ligand, 4,4'-dicarboxy-2,2'-bipyridine ( $\text{H}_2\text{dcbp}$ ), has been documented for synthesizing CPPs with different morphologies. The additives such as  $\text{Et}_3\text{N}$  and acetic acid play a vital role in the particle formation rate by means of manipulating the deprotonation rate of the organic ligand and thus the particle size and shape. In addition, the potential application of the synthesized CPPs in the antibacterial field is promising. This research demonstrates that the morphologies do have effects on the luminescent properties and antibacterial activities. Thus, in our future research work, we ought to take the morphology effect into consideration. Our research on functional coordination polymer particles is still in progress.

#### Acknowledgements

This work was supported by the National Natural Science Foundation of China (21075064, 21027013, 21021062 and 90813020) and the National Basic Research Program of China (2007CB925102).

#### References

- W. Cho, H. J. Lee and M. Oh, *J. Am. Chem. Soc.*, 2008, **130**, 16943.
- L. H. Wee, S. R. Bajpe, N. Janssens, I. Hermans, K. Houthoofd, C. E. A. Kirschhock and J. A. Martens, *Chem. Commun.*, 2010, **46**, 8186.
- M. Oh and C. A. Mirkin, *Angew. Chem., Int. Ed.*, 2006, **45**, 5492.
- M. Oh and C. A. Mirkin, *Nature*, 2005, **438**, 651.
- P. Horcajada, C. Serre, M. Vallet-Regí, M. Sebban, F. Taulelle and G. Férey, *Angew. Chem., Int. Ed.*, 2006, **45**, 5974.
- A. M. Spokoiny, D. Kim, A. Sumrein and C. A. Mirkin, *Chem. Soc. Rev.*, 2009, **38**, 1218.
- P. Horcajada, T. Chalati, C. Serre, B. Gillet, C. Sebrie, T. Baati, J. F. Eubank, D. Heurtaux, P. Clayette, C. Kreuz, J.-S. Chang, Y. K. Hwang, V. Marsaud, P.-N. Bories, L. Cynober, S. Gil, G. Férey, P. Couvreur and R. Gref, *Nat. Mater.*, 2010, **9**, 172.
- W. J. Rieter, K. M. L. Taylor, H. An, W. Lin and W. Lin, *J. Am. Chem. Soc.*, 2006, **128**, 9024.
- R. McHale, N. Ghasdian, Y. Liu, M. B. Ward, N. S. Handow, H. Wang, Y. Miao, R. Brydson and X. Wang, *Chem. Commun.*, 2010, **46**, 4574.
- Z. Ni and R. I. Masel, *J. Am. Chem. Soc.*, 2006, **128**, 12394.
- Z. L. Wang, W. H. Fang and G. Y. Yang, *Chem. Commun.*, 2010, **46**, 8216.
- Q. Lu, F. Gao, D. Li and S. Komarneni, *Adv. Tech. Materials and Mater. Proc. J.*, 2005, **7**, 111.
- J. Yang, B. Li, G. F. Ma, Y. Y. Liu and J. P. Zhang, *Chem. Commun.*, 2010, **46**, 8383.
- K. Liu, H. P. You, Y. H. Zheng, G. Jia, L. H. Zhang, Y. J. Huang, M. Yang, Y. H. Song and H. J. Zhang, *CrystEngComm*, 2009, **11**, 2622.
- T. Tsuruoka, S. Furukawa, Y. Takashima, K. Yoshida, S. Isoda and S. Kitagawa, *Angew. Chem., Int. Ed.*, 2009, **48**, 4739.
- Y. Su, M. Hu, C. Fan, Y. He, Q. Li, W. Li, L. Wang, P. Shen and Q. Huang, *Biomaterials*, 2010, **31**, 4829.
- A. D. Russell and W. B. Hugo, *Prog. Med. Chem.*, 1994, **31**, 351.
- W. Hu, C. Peng, W. Luo, M. Lv, X. Li, D. Li, Q. Huang and C. Fan, *ACS Nano*, 2010, **4**, 4317.
- R. Kumar and H. Münstedt, *Biomaterials*, 2005, **26**, 2081.
- E. Tynan, P. Jensen, P. E. Kruger, A. C. Lees and M. Nieuwenhuysen, *Dalton Trans.*, 2003, 1223.
- E. Tynan, P. Jensen, A. C. Lees, B. Moubaraki, K. S. Murray and P. E. Kruger, *CrystEngComm*, 2005, **7**, 90.
- X. Yang, F. Lai, J. Zhang and Q. Chen, *J. Phys. Chem. C*, 2009, **113**, 7123.
- D. Tanaka, A. Henke, K. Albrecht, M. Moeller, K. Nakagawa, S. Kitagawa and J. Groll, *Nat. Chem.*, 2010, **2**, 410.
- H. J. Lee, W. Cho and M. Oh, *CrystEngComm*, 2010, **12**, 3959.
- Y.-M. Jeon, G. S. Armatas, D. Kim, M. G. Kanatzidis and C. A. Mirkin, *Small*, 2009, **5**, 46.
- H. J. Lee, W. Cho, S. Jung and M. Oh, *Adv. Mater.*, 2009, **21**, 674.
- K. Bhar, S. Choubey, P. Mitra, G. Rosair, J. Ribas and B. K. Ghosh, *J. Mol. Struct.*, 2011, **988**, 128.
- S. Wang, L. Zhang, G. Li, Q. Huo and Y. Liu, *CrystEngComm*, 2008, **10**, 1662.
- H. Jung, D. Lee and K. Y. Jung, *J. Alloys Compd.*, 2005, **390**, 189.
- S. Oshio, K. Kitamura, T. Shigeta, S. Horii, T. Matsuoka, S. Tanaka and H. Kobayashi, *J. Electrochem. Soc.*, 1999, **146**, 392.
- J. Meletiadis, J. F. Meis, J. W. Mouton, J. P. Donnelly and P. E. Verweij, *J. Clin. Microbiol.*, 2000, **38**, 2949.
- A. Tavman, I. Boz and A. S. Birteköz, *Spectrochim. Acta, Part A*, 2010, **77**, 199.
- B. Prathima, Y. S. Rao, S. A. Reddy, Y. P. Reddy and A. V. Reddy, *Spectrochim. Acta, Part A*, 2010, **77**, 248.
- K. Yamamoto, S. Ohashi, M. Aono, T. Kokubo, I. Yamada and J. Yamauchi, *Dent. Mater.*, 1996, **12**, 227.